Seismicity and deformation at convergent margins due to heterogeneous coupling

Renata Dmowska, Gutuan Zheng, and James R. Rice

Division of Applied Sciences and Department of Earth and Planetary Sciences, Harvard University, Cambridge, Massachusetts

Abstract. Studies of the mechanics of subduction as inferred from earthquake cycle observations suggest that the distribution and style of seismicity in the seafloor, between the trench and the outer rise, and in the slab at intermediate depth, can in some cases serve to identify asperity locations along the thrust interface [*Dmowska and Lovison*, 1992]. Such asperities, identified from seismic wavefield modeling, are the zones of highest seismic moment release in large underthrusting events. To the extent that asperity locations are relatively stationary from one event to the next, their locations provide the zones of highest expected moment release in future large earthquakes, and rupture often nucleates at the border of an asperity. The region of the thrust interface outside such asperities is, apparently, less well coupled and releases moment throughout the great earthquake cycle in some combination of aseismic creep and moderate seismicity. Thus it is reasonable that stress and deformation rates associated with the earthquake cycle should be most pronounced near asperities, and that this should have seismic and geodetic consequences. Three-dimensional finite element modeling is used here to understand such stress and deformation patterns and their variation in time, in relation to heterogeneity of coupling along thrust interfaces. The stress field helps to explain the observed clustering of seafloor seismicity along the strike of the convergent margin. In cases of convergence at approximately normal incidence, like for the region of the Valparaiso, Chile, 1985 thrust event, the modeling is consistent with the observation that areas of large earthquakes in the seafloor toward the outer rise and in the slab tend to lie within corridors through thrust zone asperities, running perpendicular to the line of the trench. We seek to learn if such model stress fields are consistent with observations, for the strongly oblique subduction margin of the Rat Islands, western Aleutians, 1965 event, that active areas of the outer rise and slab at intermediate depth are offset along strike from asperity locations. Modeling results here for the stress in the seafloor raise the possibility that to explain this offset, the asperity zones along the thrust interface may have to be strung out along the direction of oblique slip, perhaps reflecting the contact path of subducting seamounts or geometric irregularities along the interface. Shear stress patterns created in the upper plate, when there is oblique subduction, suggest that favorable areas for back-arc strike slip activity following underthrusting, as in the Adak Island, central Aleutians, region of the 1986 Andreanof Island earthquake [*Ekström and Engdahl*, 1989], will also be shifted along strike from asperity locations. Our analyses show how deformation patterns on the earth's surface above asperities differ from patterns above nonasperities, and hence provide tools to identify inhomogeneous coupling from geodetic observations. We discuss possible bathymetric, topographic, and structural signals of strength of coupling, and of asperities, particularly noting that the density and extent from the trench of seafloor normal faults correlates with seismically inferred zones of strongest coupling in the central Aleutians.

Introduction

Studies of seismicity near subduction margins, in the outer rise as well as at intermediate-depth [*Christensen and Ruff*, 1983, 1986, 1988; *Astiz et al.*, 1988; *Dmowska et al.*, 1988; *Dmowska and Lovison*, 1988; *Lay et al.*, 1989], provide evidence that there is time dependence of the style of seismicity in large regions adjacent to a strongly coupled thrust interface. The time dependence is illustrated in Figure 1, from *Lay et al.* [1989], which shows when compressional (solid symbols) and extensional (open symbols) events have

occurred relative to the time of a large or great earthquake, the magnitude of which is given on the vertical axis. Such results seem consistent with expected patterns of stress accumulation and release in the earthquake cycle of the adjacent thrust interface, both as understood qualitatively and as represented in elementary models [*Dmowska et al.*, 1988, *Rice and Stuart*, 1989, *Taylor et al.*, 1996] of stress and deformation associated with the earthquake cycle.

Outer rise response. The outer rise region of the seafloor is loaded in extension by a great thrust event, and most of the extensional seismicity there occurs within a few years of the event (Figure 1). As the cycle matures, ongoing plate motion and mantle flow processes cause the stress to change toward compression and, in some places, that results in the relatively rare compressional outer rise
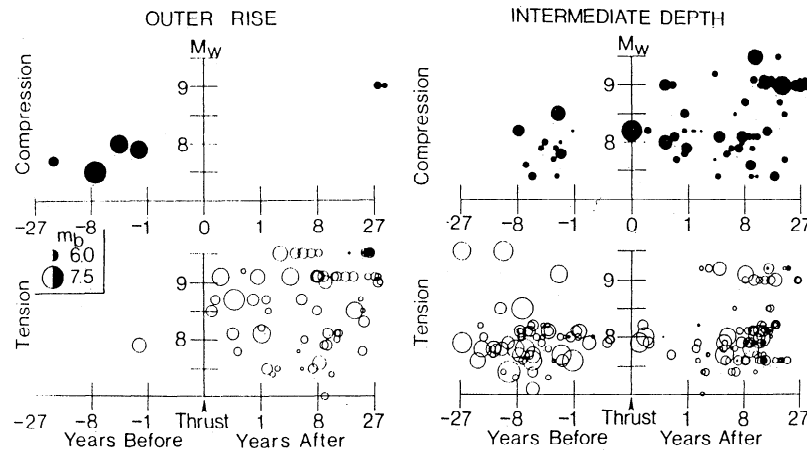
Figure 1. From *Lay et al.* [1989]: Composite plots of outer rise earthquakes on the left, and slab earthquakes at intermediate depth on the right. Earthquake times are shown relative to the time of a large or great thrust event on the adjacent interface, and the moment magnitude of that event is plotted on the vertical axes. Upper panels (solid symbols) are for compressional events and lower (open symbols) for extensional; symbol sizes scale with earthquake magnitudes.

events. The outer rise events in this data set occur typically within 0 to 75 km of the trench [see *Masson*, 1991] so, evidently, stress fluctuations associated with the great earthquake cycle give observable effects, even at distances up to 75 km or so from the trench. In fact, the outer rise events discussed fall between the trench and the topographic high to which the name "outer rise" strictly refers. They would more accurately be called "pretrench" or "outer trench slope" events. We keep the accepted terminology of outer rise events here, understanding it to refer to events in the sloping seafloor between the trench and the topographic high. Elastic models of plate bending in a subducting seafloor, based on a plate on an elastic foundation, do suggest that bending stresses are higher at some or all such outer slope locations than at the topographic high, at least when we assume that the plate edge at the trench is loaded by any combination of a downward transverse shear force and a bending moment of the same sense as that at the high. In fact, it may be shown that for all such loading combinations, maximum bending stress occurs in the elastic model at some location between the trench and a third of the distance to the high.

The two-dimensional finite element calculations by *Rice and Stuart* [1989] and *Taylor et al.* [1996] suggest that the cycle-related extensional stress fluctuations, which are to be superposed on the bending stresses, at the locations of the outer rise events range over only 1 to 5 bars. The magnitude is even smaller when the shallow part of the thrust zone, adjoining the trench, is taken to be aseismic (*Taylor et al.*, 1996). Figure 2, adapted from a similar diagram from *Dmowska and Lovison* [1988], but now introducing considerations of strength envelopes and non-elastic bending [*McAdoo et al.*, 1978; *Goetze and Evans*, 1979], shows our understanding of how such small stress changes can be influential. It also illustrates our viewpoint on earthquake-cycle-related induction of seismicity, namely, that the (generally small) time-dependent stress fluctuations associated with the cycle modulate the time-averaged stress distribution in a region and hence can turn on or off a type of seismicity which is, itself, determined by that time-

average stress state. In the seafloor between the trench and the outer rise, that time-average stress state is expected to define a bending stress field which is typically close to extensional failure at shallow depths, and may in some places be close to compressional failure at greater depths, or perhaps to both, as illustrated on the left in Figure 2. The calculated stress fluctuations associated with the earthquake cycle are found to amount principally to horizontal extension or compression in the outer rise (*Taylor et al.* 1996), as on the right (and greatly exaggerated relative to the bending stresses) in Figure 2. It is these small stress fluctuations which modulate the effects of the time-average bending stress state, and hence control the timing and type of seismicity produced in the outer rise.

Since the outer rise is a significant indicator of coupling and (as discussed below) its heterogeneity along strike, it is important to know what factors cause the outer rise in a given area to be prone to induction of shallow extensional failures, or to the rarer and more deeply nucleating compressional failures, or perhaps to both. Compressional failures are of great interest because of their role as
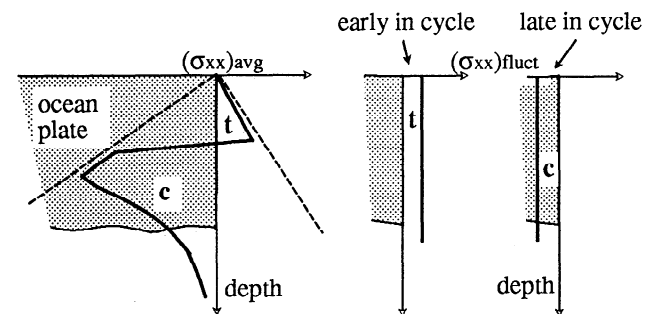

Figure 2. Stress state in the outer rise and superposed effect of stress fluctuations in the earthquake cycle, modified from *Dmowska and Lovison* [1988] to include strength envelopes. *Left plot:* Time-average stress state for bending of seafloor between trench and outer rise (stress locally near failure). *Right two plots:* Stress fluctuations (exaggerated) associated with subduction earthquake cycle.

intermediate term precursors to great thrust events [*Christensen and Ruff*, 1986, 1988; *Dmowska and Lovison*, 1988]. In a previous survey of seismic behavior of the outer rise [*Christensen and Ruff*, 1988; *Dmowska and Lovison*, 1990], we could not find cases for which a given region was known to show both large extensional and compressional outer rise activity, i.e., at magnitude levels above about $m_b = 5.5$. Rather, the general pattern was that either large tensional failures occurred after the thrust event or, less frequently, large compressional failures occurred before, but not both. Thus it may be valuable to reexamine elastic (Coulomb) plastic descriptions of bending and stress in the outer rise [*McAdoo et al.*, 1978; *Goetze and Evans*, 1979; *McNutt and Menard*, 1982], seeking to understand what conditions of age, convergence rate, dip and other features of the margin could cause the deeper compressive part of the bending stress field to indeed be close to compressional failure, like in Figure 2, rather than to be attenuated by ductile creep.

Slab at intermediate depth. There is similar but less clear cycle dependence of the rate and style of seismicity in the slab at intermediate depth, Figure 1, but now developing into increased extensional activity as the cycle matures. This is thought to reflect gravitational pull from the cold descending slab, an extensional effect which gets reduced, and in some cases reversed to compression, by large events on the thrust interface. *Taylor et al.* [1996] provide a fuller discussion of fluctuations of stress states in the slab induced by great earthquake cycles. Now interpretation of the effect of perturbations is less straightforward than for the outer rise: While the time-average stress field is thought to be dominated by slab pull, it is also complicated by unbending, thermal stress, and probably dehydration. Also, the fluctuations in several components of stress are important to contributing to failure in the slab and we cannot limit attention just to horizontal extensional stress as seems appropriate in the outer rise. Still, slab seismicity at intermediate depths does show strong signs of being related to coupling on the thrust interface.

Clustering of Seismicity in Association With Asperities

An important observation about the outer rise and slab seismicity just discussed is that the zones which respond by such seismicity to stress fluctuations of the great earthquake cycle are not distributed uniformly along the subducting margin. Rather, they cluster along strike [*Dmowska and Lovison*, 1992]. From studies of the zones of the large subduction events of Rat Islands 1965, Alaska 1964 and Valparaiso 1985, *Dmowska and Lovison* [1992] were able to further show that this clustering occurs in association with locations along the thrust interface that had been independently identified as "asperities," from the modeling of seismic waveforms radiated during the great ruptures. These asperities are the areas of highest slip in the large underthrusting event. It is plausible to interpret the asperities as also denoting the regions of the thrust interface which are most firmly locked between great earthquakes, that is, as the regions which are most strongly coupled, in the sense of showing the lowest interseismic slip rates. Other parts of the interface slip more throughout the earthquake

cycle, in some mixture of aseismic creep and moderate seismicity. Thus it is reasonable that effects of stress changes in the earthquake cycle should indeed be more pronounced near the asperities than near less well locked portions of the interface. This observation relates the appearance of trench outer rise seismicity to the large scale inhomogeneities in interplate coupling along the convergent margin.

The active zones in the outer rise and in the slab at intermediate depth might be expected to be located adjacent to the highest slip region on the interface, along a corridor through it running perpendicular to the trench. Such is observed near the Valparaiso 1985 zone which is one of only moderately oblique convergence. That is illustrated in Figures 3a and 3b where Figure 3a, from *Dmowska and Lovison* [1992], shows the aftershock zones (dashed lines) of, from the north, the 1943, 1971, and 1985 underthrusting earthquakes in central Chile. The black symbols denote epicenters of all the large earthquakes (with $m_b \geq 5.6$) located west of the aftershock zones in the outer rise area, and east of them at depths more than 45 km (i.e., in the slab), for the period January 1, 1964, to March 3, 1985, that is, for the 20-year period before the Valparaiso earthquake of March 3, 1985. The event in the outer rise, with CMT mechanism marked next to it, is the compressional event of October 16, 1981 ($M_S=7.2$). Figure 3b shows the slip (in centimeters) in the 1985 Valparaiso underthrusting event, projected to the surface of the Earth, as inferred in the seismic inversion by *Mendoza et al.* [1994]. We see that the outer rise compressional event of 1981 locates adjacent to the region of greatest slip in 1985. There is also a cluster of three large events to the east, at intermediate depths in the descending slab. A line drawn from the outer rise event to the centroid of the cluster of three would pass through the largest slip contour shown, encircling the 1985 epicenter, suggesting an association of the events with the asperity location that our modeling, to be discussed, supports. The southernmost event in the slab may possibly be related to the secondary high slip area in 1985, shown to the south in Figure 3b. All these earthquakes occurred before the Valparaiso event and could, with considerable uncertainty, be regarded as forecasting aspects of its moment distribution. The northernmost cluster of four events are most likely associated instead with the 1971 rupture; *Dmowska and Lovison* [1992] noted that there was a cluster of lower magnitude extensional failures in the outer rise at comparable latitude following that event.

Similar clustering of outer rise seismicity in association with the areas of highest slip in the subduction events has been observed for the Alaska 1964 and Rat Islands 1965 segments studied by *Dmowska and Lovison* [1992], but we shall see that the situation is more complex in regions of significantly oblique subduction like for the Rat Islands 1965 zone.

This evidence of an association between asperities on the thrust interface and seismic activity in the adjacent regions is the motivation for our modeling work reported here. Such modeling should help to understand induction of seismicity in the outer rise and in the slab at intermediate depth in association with heterogeneous coupling along the thrust interface and also provide a basis for interpreting related seismic and geodetic signals in the overlying plate. Here our primary focus in the modeling is on understanding outer
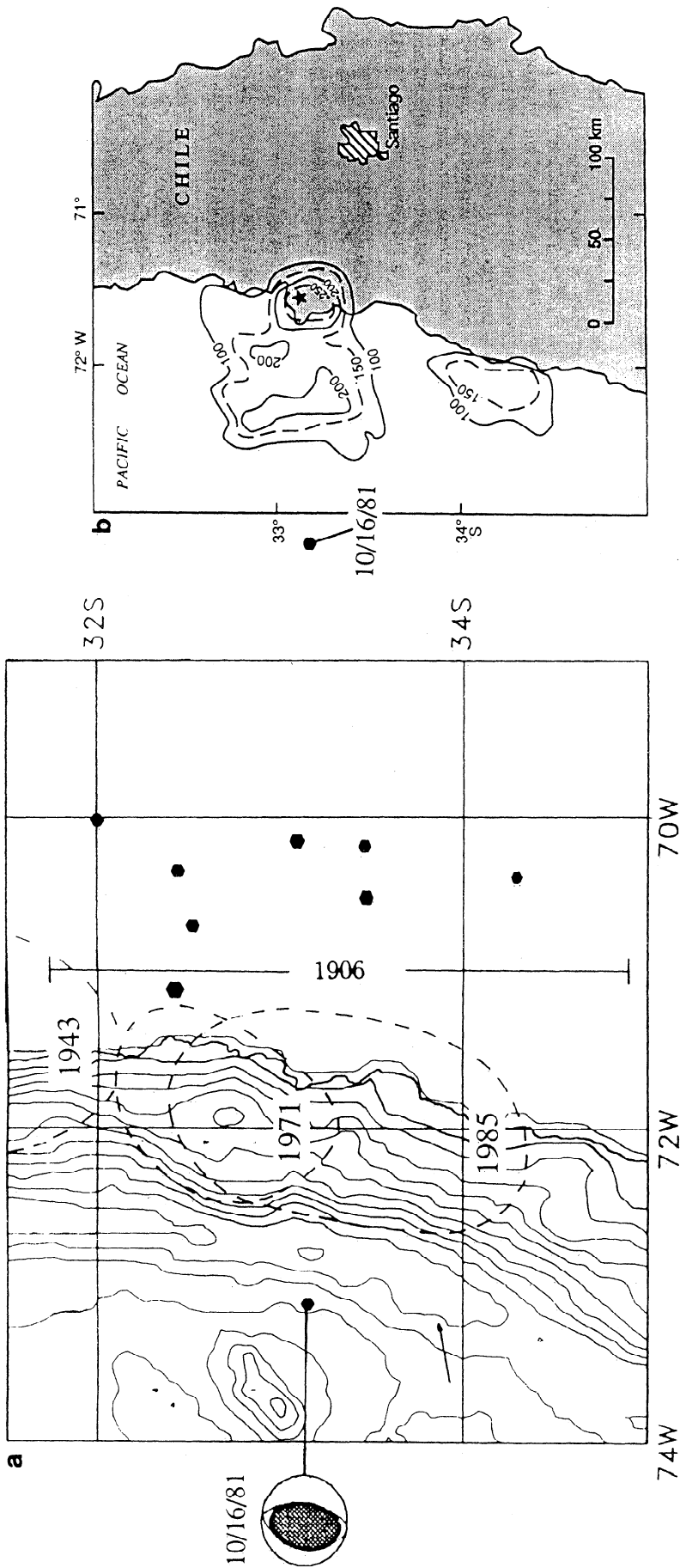
Figure 3. (a) Events with mb > 5.6 in the outer rise and in the slab at intermediate depth over the 20 years prior to the Valparaiso underthrusting earthquake of March 3 1985, from *Dmowska and Lovison* [1992]. (b) Slip contours, in units of cm, projected to the Earth's surface, from seismic inversion of the 1985 event, from *Mendoza et al.* [1994].

rise seismicity. We also discuss structural, bathymetric, and topographic features in terms of coupling and its heterogeneity.

Finite Element Modeling of Stress And Deformation

To better understand the temporal and spatial variation of seismicity, we present here some simplified models of earthquake cycles in subduction segments with inhomogeneous locking along strike. We do so by analyzing space- and time-dependent stressing and deformation associated with earthquake cycles in a three-dimensional finite element model (Figure 4a) of a subducting margin with a row of asperities (three-dimensional case of Figure 4b, also Figures 5 and subsequent). Previous
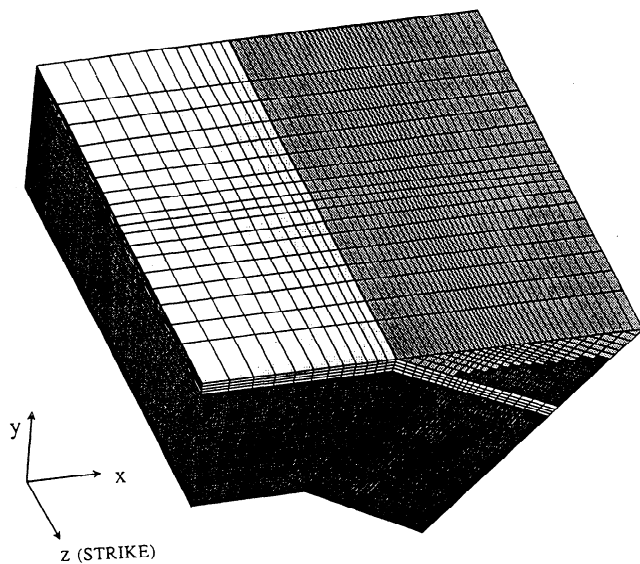
(a)
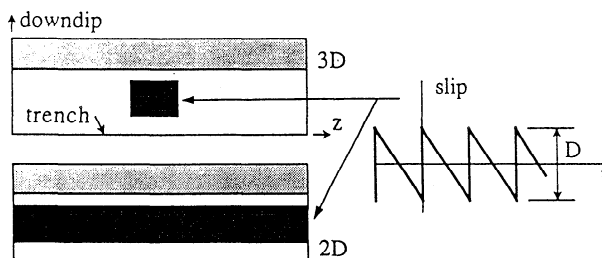
(b)

Figure 4. (a) Three-dimensional finite element mesh for subduction zone analysis; z direction is along strike, parallel to the margin, x direction is perpendicular to the margin and parallel to Earth surface, pointing toward the over riding plate. (b) Thrust interface in three- and two-dimensional interpretations of the model. The asperity regions are shown in black and, to calculate the fluctuating part of the stress history associated with periodically repeated earthquakes, the sawtooth slip history shown is imposed on them. White regions outside asperities are freely slipping.

modeling of stress variations in the earthquake cycle [*Dmowska et al.*, 1988, *Rice and Stuart*, 1989, *Taylor et al.*, 1996] treated the subduction process as if it was uniform along strike and hence ignored the heterogeneity of the seismic coupling. All regions in the subducting and upper plates and mantle, outside the thrust interface, are assumed to respond elastically to stress fluctuations caused by the thrust zone earthquakes in the three-dimensional work that we report here. However, we know from our experience in two-dimensional modeling of crustal deformation in the Shumagin Islands region [*Dmowska et al.*, 1992; *Zheng et al.*, 1996] that viscous relaxation in the mantle wedge, and along the downdip extension of the seismically coupled zone, can significantly influence surface deformation and its time dependence. We use here models with highly simplified free-slip, or kinematically imposed slip, conditions along the interface outside the asperity. For the future, it will be important to explore more options for time-dependent material response there and generally to analyze relaxational effects more fully; that is demanding of computer time and storage.

The section considered in Figure 4a is given periodic boundary conditions at its ends, along strike, consistent with periodically replicating that section along the convergent margin. The interplate interface in each section has one or two asperities, which are highly coupled areas where the slips in repeated earthquakes are prescribed. Results shown are for a fixed dip of 25° as well as fixed plate thicknesses.

We impose great earthquake slips on the asperities and calculate stress and displacement elsewhere, including elsewhere along the thrust zone outside the asperities. We use the following simplified models for the thrust interface outside the asperities: freely slipping models, for which slip is calculated outside the asperities so as to assure that there is no change in shear stress there during rupture or throughout the cycle, and mixtures of freely slipping and kinematically dislocated models which provide a coseismic drop in stress there during the event (although not as much as within the asperities). Resulting deformation reflects the cycle-related changes caused by identically repeated subduction events, and is the response to the standard "sawtooth" time history of slip [e.g., *Dmowska et al.*, 1988; *Taylor et al.*, 1996] thus imposed at the asperities. This modeling actually solves for the fluctuating part of the stress field due to repetitive earthquakes on the asperities. Following *Dmowska et al.* [1988] and *Taylor et al.* [1996], we imagine a reference state for the calculation in which the seafloor steadily subducts into the mantle, and for which the spatial distributions of stress and particle velocity are independent of time. We then solve for the fluctuation of stress and deformation from that reference state due to the fact that slippage along coupled parts of the fault does not occur at a steady rate, but rather as stick-slip events. Hence the "staircase" history of slip versus time on the asperities becomes, for purposes of analyzing the fluctuating part of the stress/deformation field, the well-known "sawtooth" slip versus time history used as a kinematically imposed boundary condition for such studies (Figure 4b). The simplification is made, in modeling of this type, that material constitutive response to the fluctuating field outside the thrust interface is assumed to be linear. That response is taken as linear elastic in regions like the ocean floor and

slab core which are not expected to relax on the earthquake cycle timescale but is sometimes taken as linear (Maxwell) viscoelastic in relaxing regions of the mantle, mantle wedge, and aseismic downdip continuation of the fault zone. Here we take the response as elastic in all such regions; *Taylor et al.* [1996] report results of viscoelastic modeling, for the two-dimensional case.

The sawtooth slip history is accomplished by imposing a corresponding history of shear "transformation" strain within the layer of elements representing the asperity part of the fault. This is readily done within the ABAQUS finite element program that we use, which allows users to specify arbitrary thermal "expansion" tensors. Thus we create a material which shears when subjected to a change in "temperature," where temperature now becomes just a measure of the extent of the shear transformation, or slip, along the asperity. The modeling gives, as a calculated response, the slip on the thrust interface outside the asperity region at the times of the imposed asperity slips, and throughout the cycle time between them. The simplest case is that of free slip outside the asperity. That is accomplished in the finite element method by greatly reducing the elastic shear modulus μ_f of the layer of elements representing the fault zone outside the asperities, but increasing the Poisson ratio there so that the bulk modulus is unchanged. If the fault layer in the finite element mesh has thickness h, and if W is a linear dimension, measured downdip, of the region which is to undergo free-slip, then we simulate free-slip by reducing μ_f in that region so that $\mu_f \ll \mu \, h \, / \, W$, where μ is the modulus of the surrounding material.

We modify this free-slip model in a simple way so as to cause the thrust region outside the asperity zone, but over the same depth range, to undergo nonzero cycle-related shear stress changes. We do so by adding a uniform-along-strike thrust-interface dislocation to the three-dimensional free-slip model. Here we wish to represent the idea that slips outside the asperity will, we think, typically involve a real stress drop. We observe that the modeling by *Rice and Stuart* [1989] and *Taylor et al.* [1996] involved uniformly imposing slip along the thrust interface, thus achieving a distribution of stress drop that was uniform along strike (although not uniform with depth). Such a two-dimensional case corresponds to the lower case in Figure 4b, for which the "asperity" region extends uniformly along strike. Thus, for this modification, we add together the stress and deformation results of the three-dimensional asperity model with free slip outside, and the two-dimensional model with slip over the asperity depth range that is uniform along strike. That is, the two-dimensional model is chosen so that its coupled zone has the same downdip width as the asperity in the three-dimensional model, with free-slip above towards the trench and somewhat below. By varying the relative contribution of slip on the isolated asperity in the three-dimensional free-slip model, and of uniform slip along strike in the two-dimensional model, we can create a class of models which span the extremes from no stress drop outside asperities to uniformity of stress drop along strike.

That is, if $\{\sigma\}_{3D}$ and $\{u\}_{3D}$ are the three-dimensional stress and displacement field in the solution with free-slip outside the asperity, and if $\{\sigma\}_{2D}$ and $\{u\}_{2D}$ are the two-dimensional fields for imposed slip on the interface that is uniform along strike (and the same magnitude as imposed on

the asperities in the three-dimensional free-slip solution), as in the lower case of Figure 4b, then we represent this class of solutions as

$$\{\sigma, u\} = f \, \{\sigma, u\}_{3D} + (1-f) \, \{\sigma, u\}_{2D} \, ,$$

where the factor f determines a member of the class. Factor $f = 0$ corresponds to uniform stress drop along strike, and $f = 1$ to a stress drop that vanishes everywhere outside the asperity.

Stress and Deformation Fields

Results of interest, relating to the nonuniformity of locking along strike, include the space- and time-dependent stress and deformation of the upper plate, which will in some cases be accessible for geodetic measurements, as well as the stressing of the area of the outer rise and descending slab, with their sometimes pronounced cycle-related seismicity. Figures 5 and 6 show contour plots of stress changes (component σ_{xx}, perpendicular to trench) on the Earth's surface due to an earthquake for, respectively, the one (Figure 5a) and two (Figure 6a) asperity cases. The horizontal axes in Figures 5 and 6 run along the strike of the margin, that is, the z direction. The vertical axes in the figures correspond to direction x, along the Earth's surface perpendicular to the trench, with negative values of x corresponding to the pretrench and outer rise zones in the subducting plate, and positive to the over riding plate. Stress contour intervals are $\Delta\sigma_{xx} \, W \, / \, \mu \, D \approx 0.014$, where D is the slip on the asperity in each earthquake, W the nominal thrust interface width (100 km), and μ the elastic shear rigidity. Regions where there is cross-hatching are of negative (i.e., compressive) stress change. Regions without cross-hatching are of positive (extensional) change and so, wherever they coincide with a region of extensional normal faulting, those stress changes would encourage seismicity on mature faults. In the cases of Figures 5b and 6b the interplate interface outside the asperity is freely slipping, corresponding to $f = 1.0$ above. In Figure 5c we have used $f = 0.75$ so that the slip on the asperity is approximately 4 times the slip at locations very far away along strike (i.e., if we imagine the section in Figure 4 to extend indefinitely far along strike); that slip ratio is $1 \, / \, (1-f)$ for general f.

Figures 5 and 6 reveal that an asperity creates a corridor, extending from the outer-rise into the upper plate (and also into the subducting slab at intermediate depth), in which the most prominent cycle-related effects on seismicity and surface deformation would be expected to be confined. In particular, both Figures 5 and 6 show a region on the oceanic plate, in the area between the trench and the outer rise, where the highest stress variations associated with the earthquake cycle occur. It is positioned in front of the asperity. It is also interesting that the stress change in all (Figure 5b) or much (Figure 5c) of the outer rise away from that channel is very slightly negative, and thus would discourage extensional seismicity, making it likely that activity in the outer rise would be confined to the sort of corridor mentioned. The figures show stress changes immediately following earthquakes and are most directly relevant to outer rise extensional events after great underthrusts. However, to the extent that the mantle
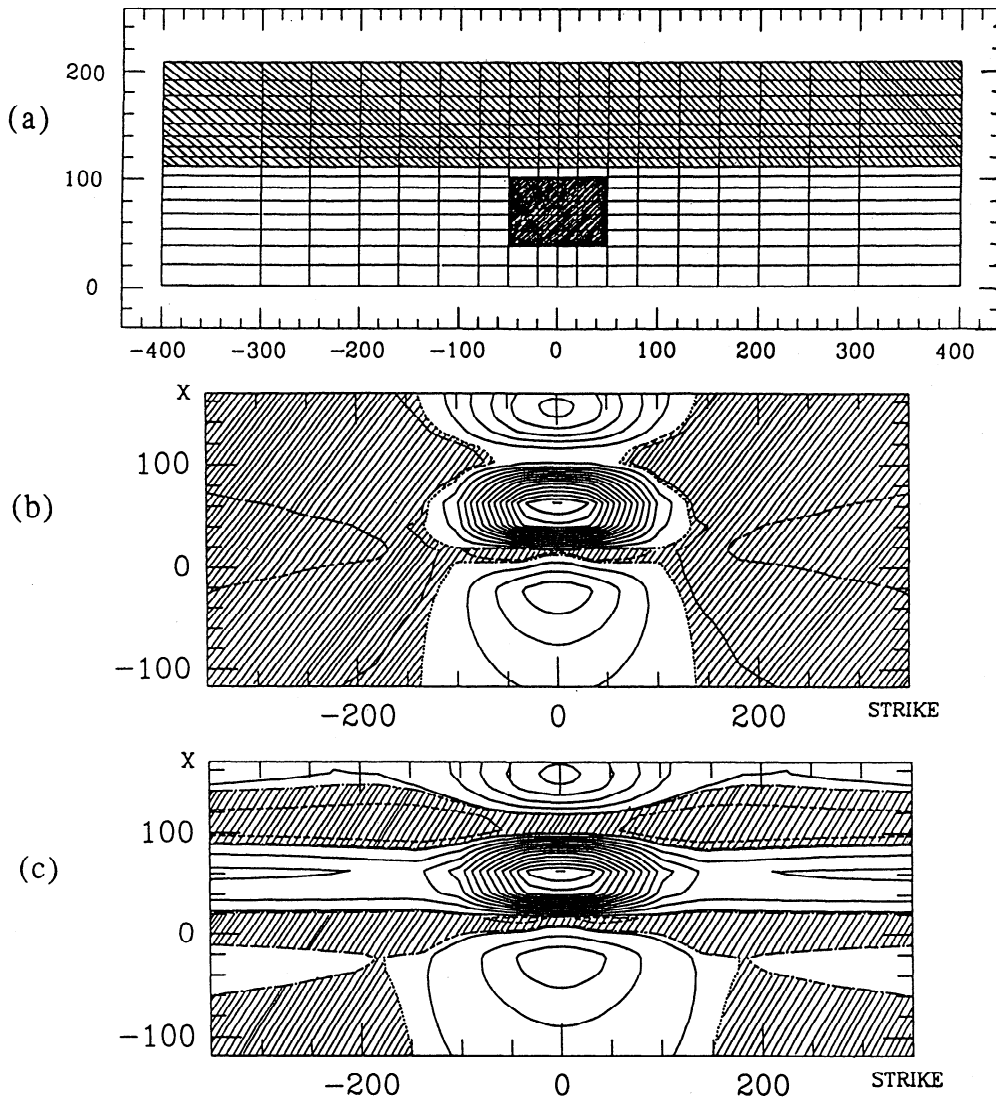
Figure 5. (a) Position of asperity on the thrust interface; orientation like in Figure 4b; distances in km. (b) Change σ_{xx} in extensional stress in direction perpendicular to trench near the Earth's surface, negative (compressional) where cross-hatched, due to slip by D on the asperity, for case with freely-slipping thrust interface outside the asperity (f = 1.0). The contour intervals are $\Delta\sigma_{xx}$ W / μ D = 0.014. (c) Change σ_{xx} in extensional stress for case with added uniform dislocation along strike, such that slip within the asperity is about 4 times the slip at locations far away along strike (i.e., f = 0.75). The contour intervals are $\Delta\sigma_{xx}$ W / μ D = 0.013 .

relaxation is neglected, the fluctuating part of the stress that our procedure computes varies linearly in time through the cycle and averages to zero. Thus the same contour plots in Figures 5 and 6, with the signs of the stress changes reversed, also show the fluctuating part of the stress field just before the next large event. Hence that late-cycle stress perturbation is also concentrated in front of the asperity, and along a corridor through it, as we consider to be the case for the events near Valparaiso in Figure 3.

Figure 6 also provides an understanding of how widely separated asperities can interact with the loading of the portions of the margin between them. Figure 7 is for the single asperity case, again with freely slipping interface outside. It shows the time and space variation of the trench-perpendicular extensional stress σ_{xx}, along a line in the z direction of Figure 4, passing along strike in the upper plate above the asperity. The line corresponds to the blackened

row of elements in the insert of Figure 7, and the plot is of σ_{xx} as a function of time throughout a complete earthquake cycle (duration T_{cyc}) and of distance along strike. This and similar plots that we have made for other rows emphasize that the channeling of effects of the asperity persists throughout the cycle.

Figure 8 shows contours of vertical displacement in the overlying plate associated with the thrust event, contoured in intervals Δu_y / D = 0.030 with the cross-hatched zones moving down. This is for the single asperity case. Figure 8a is for free-slip outside the asperity, f = 1 , and Figure 8b for the case f = 0.75 , the same as for Figure 5c. There is evidently strong enhancement of the cycle-related stress and deformation in the area of the upper plate positioned over the asperity. Figure 9 shows the corresponding pattern of horizontal coseismic displacement on the Earth's surface, relative to distant locations in the over riding plate. Figure
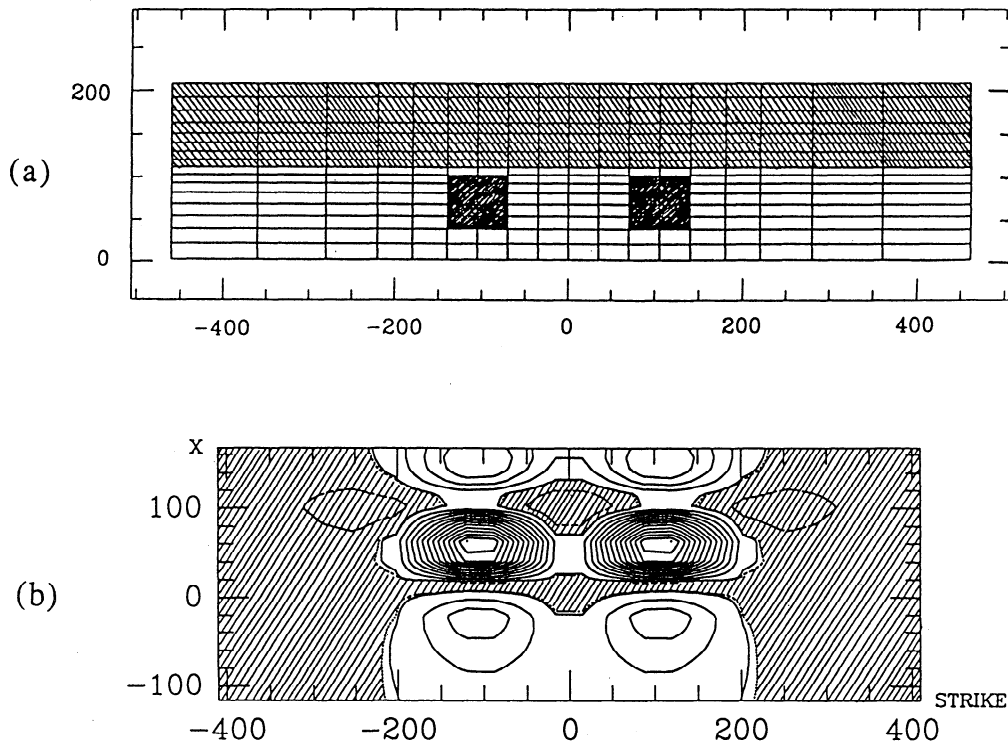
Figure 6. (a) Positions of a pair of asperities on the thrust interface; distances in kilometers. (b) Change σ_{xx} in extensional stress, negative where cross-hatched; freely-slipping thrust interface outside the asperities. The contour intervals $\Delta\sigma_{xx}\ W\ /\ \mu\ D = 0.013$.

9a is for free-slip outside the asperity, $f = 1$, and Figure 9b for the case $f = 0.75$. These model results are meaningful for interpretation of geodetic data along profiles perpendicular to the trench, and show clear differences depending on where a particular profile is positioned in relation to the underlying asperity. Strong along-strike variations of properties and thicknesses of lithological units, for example, the diminishing accreted terrain thickness from south to north for the Cascadia forearc based on seismic profiling [*Trehu et al.*, 1994], and heterogeneous layering [*Wang et al.*, 1994], can mask heterogeneities in the coupling along strike and would have to be considered in site-specific applications. The aim would be to predict geodetic signals that would follow from different assumptions about coupling distributions along the margin, to identify possible patterns that might be sought with GPS surveys to distinguish between assumptions.

Analysis of Oblique Subduction

Most convergent margins show some degree of oblique slip, and the *Dmowska and Lovison* [1992] results from the Rat Islands region of strongly oblique subduction in the western Aleutians show evidence that seismically active zones in the outer rise and in the slab at intermediate depth have a pronounced offset, along strike, from asperity locations. We have studied such oblique subduction cases, again using three-dimensional finite element modeling based on the same mesh as in Figure 4, to develop understanding of how stress fluctuations cause seismicity, and of how the

locations of observed seismicity can point to the locations of asperities on the thrust interface, when convergence is complicated by strong obliquity.

Figure 10, from *Dmowska and Lovison* [1992], shows the largest events, $m_b \geq 5.7$, in the outer rise over about 22.5 years after the February 4 1965, $M_w = 8.7$ Rat Islands earthquake. The event locations are offset from the hatched regions within the aftershock zone. Those hatched regions are taken from *Beck and Christensen* [1991, Figure 7] and are thought to be the locations of the greatest moment release (i.e., the asperities) in the Rat Islands event, as determined from analysis of P wave radiation. *Beck and Christensen* [1991] note the general consistency of their asperity locations with earlier studies and alternate methods. They also show their estimate of the distribution of moment density along strike. That has three pronounced peaks, corresponding to centers of the three hatched zones. The widths assigned to the zones are somewhat arbitrary, but indicate the breadths of the peaks. Figure 10 shows that the outer rise activity clusters to the eastern sides of the asperity locations rather than directly in front of them. *Dmowska and Lovison* [1992] showed also that activity in the slab at intermediate depths, from 25 years before to 22.5 years after the 1965 event, is instead clustered more to the western sides.

Figures 11 and 12 show results from three-dimensional finite element modeling of an obliquely subducting slab with single asperity regions on the thrust interface. The standard sawtooth slip history discussed earlier was imposed on the asperity, and the rest of the interface was allowed to freely-slip in the cases shown, i.e., $f = 1$. Now the layer of finite
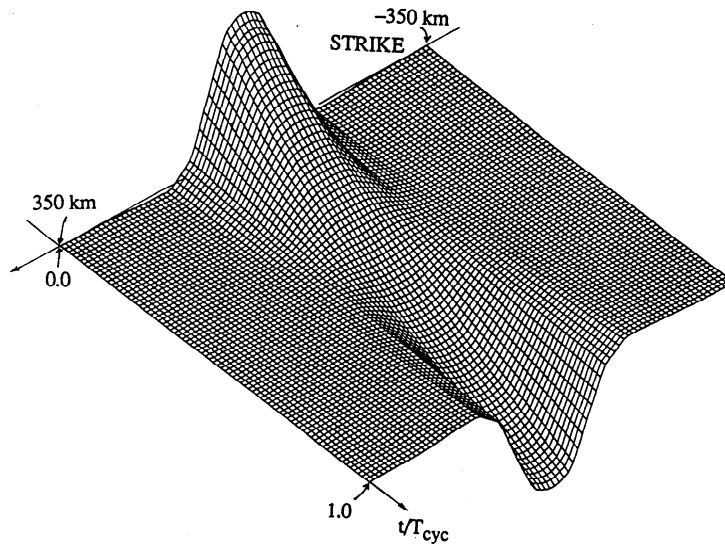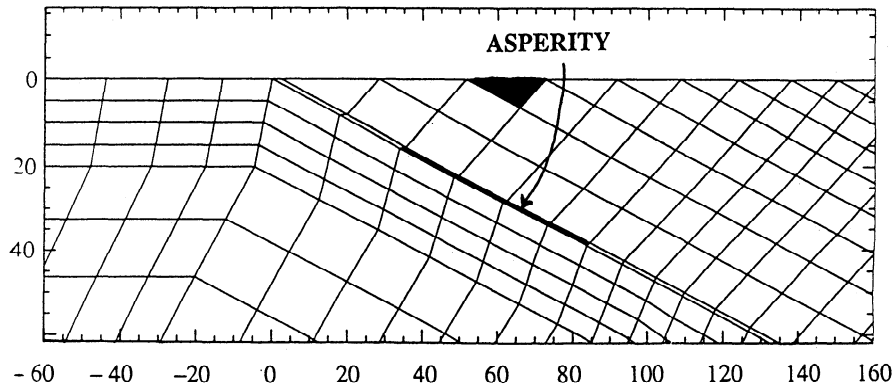
Figure 7. Fluctuating part σ_{xx} of extensional stress shown as function of time t throughout an earthquake cycle, and of distance z along strike, for the blackened row of finite elements indicated on the insert above; $t = 0$ is just after an earthquake, $t = T_{cyc}$ is just before the next one; for single asperity case of Figure 5a with freely-slipping interface outside asperity.
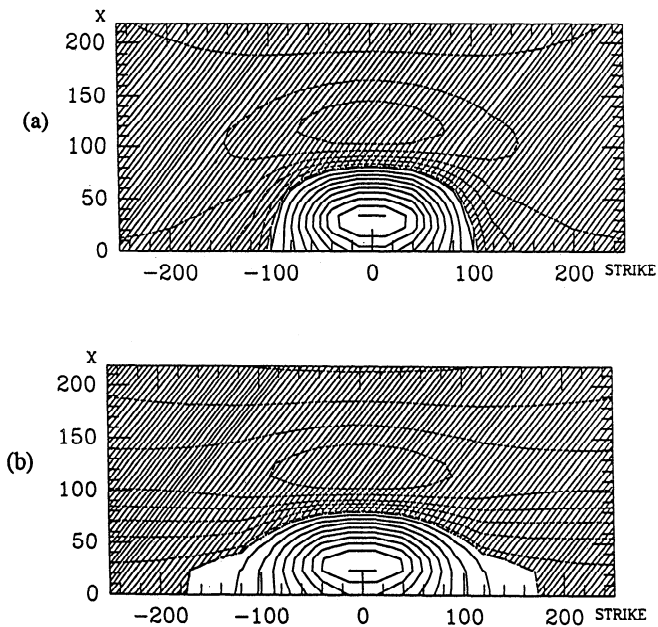
elements representing the fault zone is given transformation strains in two components of its shear strains within the asperity region, to correspond to the respective thrust and strike slip components of slip, both of which follow the sawtooth slip history and combine to model slip in the direction of the 45° line shown. In these and subsequent plots for oblique subduction, the 45° direction refers to the projection of the slip vector onto the Earth's surface. Because of the 25° dip of the interface, the slip vector direction within the interface is less steeply inclined to the direction normal to the trench, at 42.2°.

Trench-perpendicular extensional stress changes due to a thrust earthquake are contoured in Figures 11 and 12, in the

Figure 8. Uplift contours on the over-riding plate, negative (subsidence) where cross-hatched, due to earthquake slip D on the asperity; for single asperity case of Figure 5a; the contour intervals are $\Delta u_y / D = 0.030$: (a) Freely slipping ($f = 1.0$), like for Figure 5b. (b) Added uniform dislocation along strike ($f = 0.75$), like for Figure 5c.
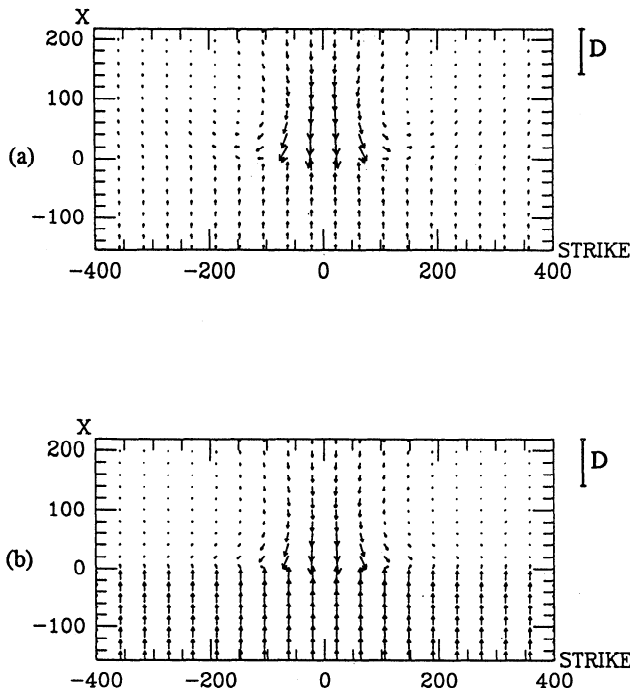
Figure 9. Horizontal displacement pattern due to earthquake slip D on the asperity; for single asperity case of Figure 5a. (a) Freely slipping (f = 1.0), like for Figure 5b. (b) Added uniform dislocation along strike (f = 0.75), like for Figure 5c.

outer rise and over riding plate, for two asperity geometries considered. Now the contours are separated by $\Delta\sigma_{xx} W/\mu$ D ≈ 0.011 and cross-hatched areas are those of negative stress change. Extensional outer rise seismicity, like in Figure 10, should be induced only where the stress changes are positive. Figure 11 is for the asperity of the same shape
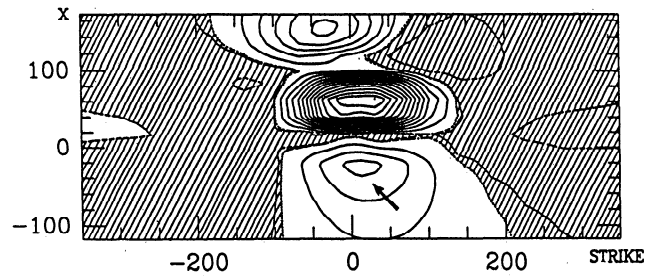
Figure 11. Change σ_{xx} in extensional stress near the earth's surface for oblique slip at 45° by amount D on the asperity of Figure 5a; freely-slipping interface outside; the contour intervals are $\Delta\sigma_{xx} W/\mu$ D = 0.011.

as in Figure 5a. We have found that the assumption of asperity shapes that are symmetric about an axis perpendicular to the trench, like for Figure 11, do not cause the locations of high cycle-related stresses to be displaced along strike quite as much as suggested by the observations in Figure 10. However, assumption of skewed asperity regions that are strung out along a path of oblique convergence, like in Figure 12a, can cause the locations of highest stress, Figure 12b, to shift distances along strike comparable to those observed. Such a skewed asperity configuration as in Figure 12a could be due to the asperity zone being formed by solid rock contact and wear debris of a subducting seamount, or by subduction of some geometric kink or other nonuniformity along the interface. These calculations were done for a 45° convergence direction, or 42.2° on the interface, as noted. A complication is that not all of the trench-parallel component of the oblique convergence vector is necessarily accommodated along the thrust interface. *Ekström and Engdahl* [1989] suggest that for the Adak Island area along the Alaska/Aleutian trench, an amount of order 40% of the trench-parallel component is
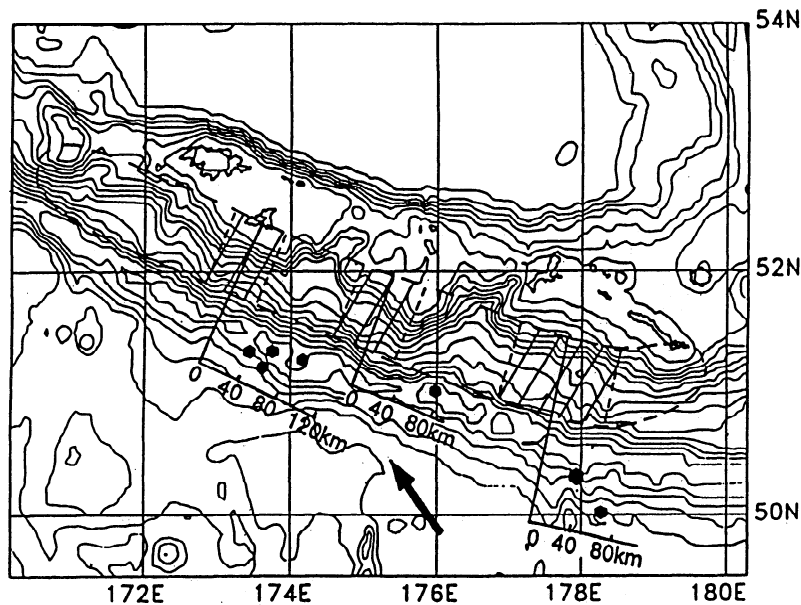

Figure 10. From *Dmowska and Lovison* [1992]: Aftershock zone (dashed line) of the February 4, 1965, Rat Islands earthquake in the Western Aleutians, with the three areas of highest moment release in the rupture, as determined by *Beck and Christensen* [1991], shown as hatched. Black symbols show the largest, m_b ≥ 5.7, of outer rise and other pretrench events occurring over 22.5-year period after the mainshock. Note offsets toward eastern sides of asperity locations.
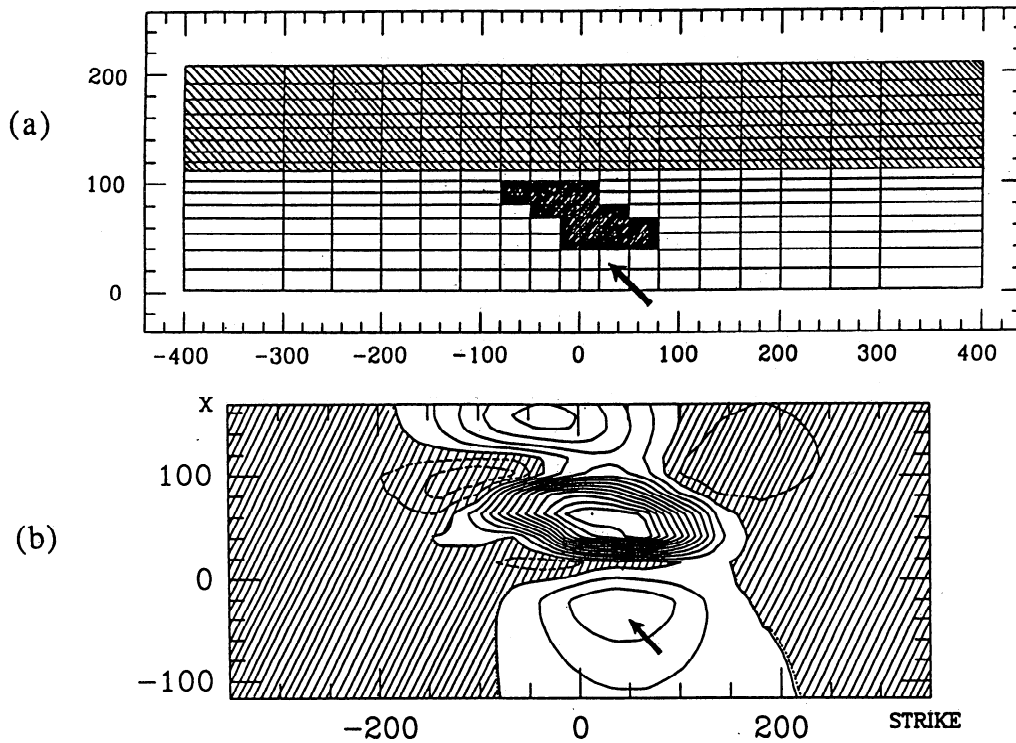
Figure 12. (a) Skewed asperity that is strung out in the direction of oblique motion. (b) Change σ_{xx} in extensional stress for oblique slip at 45° by amount D on the above asperity; freely-slipping interface outside; the contour intervals are $\Delta\sigma_{xx}$ W / μ D = 0.011 .

accommodated at the thrust interface, and the rest in back-arc strike slip activity. While the seismicity in the Rat Islands outer rise is shifted to the east of the asperities, *Dmowska and Lovison* [1992] found that seismicity in the slab at intermediate depths there is instead shifted more to the west. Figure 13 is a simplified schematic representation of how we thus expect nearby seismicity to relate to asperity locations in regions of strongly oblique subduction.

The obliquity of slip on the asperity has a pronounced effect on the pattern of coseismic horizontal displacement. This is shown for the skewed asperity geometry of Figure 12a in Figure 14, and the displacement pattern may be compared to Figure 9a.

Upper Plate and Back-Arc Seismicity

While the chief focus of studies of cycle-related seismicity has been on the outer rise and slab, like in Figure 1, we may
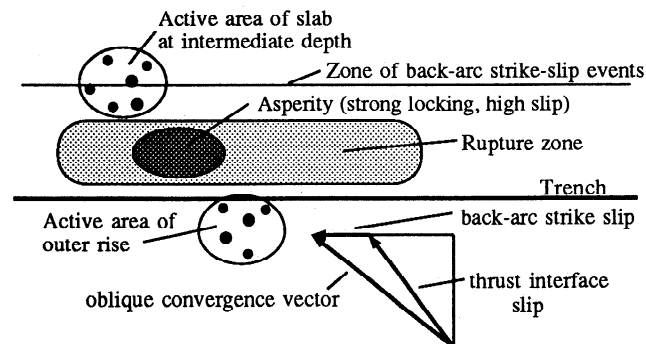
also try to explain locations of activity in the over riding plate. One data set for that is provided by the back-arc strike slip earthquakes reported by *Ekström and Engdahl* [1989] for the Adak Island region in the central Aleutians during the aftershock sequence of the May 7, 1986, M_w = 8.0 event. The observation includes five events in the crust of the upper plate (the depth is not well determined and is given as 15 km) with strike-slip mechanisms consistent with right-lateral motion on arc-parallel fault planes, and magnitudes ranging from M_w = 5.3 to 6.5, Figure 15. A slip heterogeneity (asperity) along the main interplate interface could interact with this kind of earthquake in the upper plate.

We do not yet have a specific model of that region, and there is some discrepancy in different seismological estimates of asperity locations [*Boyd et al.*, 1995]. However, Figure 16 shows contours of the right lateral shear stress σ_{zx} along the Earth's surface induced by oblique earthquake

Figure 13. Schematic of seismic activity relative to interface asperity in zone of oblique subduction.
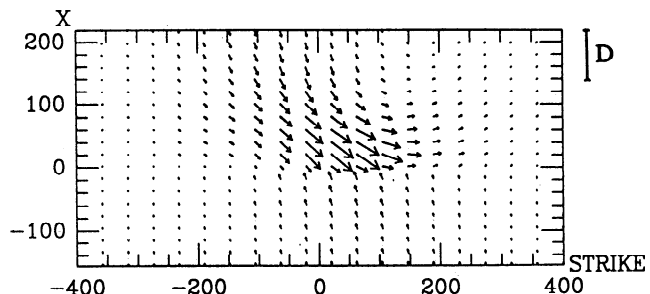

Figure 14. Horizontal displacement pattern due to earthquake slip D on the asperity, for skewed asperity of Figure 12a.
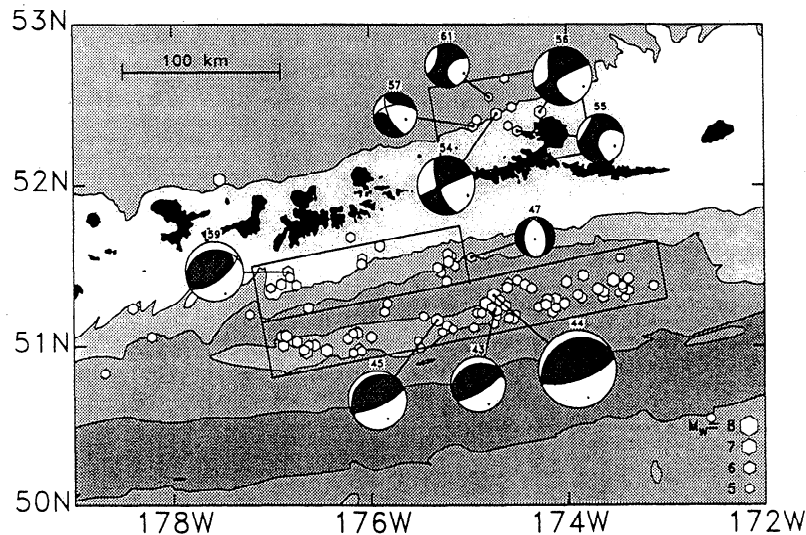
Figure 15. Back-arc strike slip activity along the Adak Island section of the Alaska/Aleutian trench, from *Ekström and Engdahl* [1989].

slip at 45° by amount D; now the contours are separated by $\Delta\sigma_{zx}$ W / μ D $\approx$ 0.015 and the stress change σ_{zx} is negative, that is, left-lateral, in the cross-hatched region. Figure 16a is for the symmetric asperity shape of Figure 5a, and the corresponding extensional stress changes σ_{xx} for that case appear in Figure 11. Figure 16b is for the skewed asperity of Figure 12a; the corresponding σ_{xx} changes for that case appear in Figure 12b. We note that the distribution of σ_{zx} is much more affected by the obliquity than is that of σ_{xx}. Also, examining the contours at the locations shown in the over riding plate which are most distant from the trench (those are not quite so far back as the *Ekström and Engdahl* [1989] strike slip locations in Figure 15), we would expect back-arc strike slip activity shortly following a great underthrust to be offset preferentially in one direction from a thrust zone asperity. Since the pattern of stress fluctuations reverses as the cycle matures, we could expect complementary regions, having negative stress change in Figure 16, to become active as the cycle matures; these are offset in an opposite sense. A complicating factor is that the contours of σ_{xx} show compression, so as to retard frictional slip, at back-arc locations where σ_{zx} is right lateral, and extension where σ_{zx} is left lateral. An important issue for further study is whether the asperity locations proposed by *Boyd et al.* [1995] and others could be shown, in terms of such stress analyses as we present here (Figures 11, 12, 16), to be consistent with the locations and timing of the *Ekström and Engdahl* [1989] events (Figure 15).

Discussion: Stationarity of Areas of Highest Coupling (Asperities)

The issue of stationarity of areas of highest seismic moment release (asperities) from earthquake to earthquake (and here we do not necessarily consider many earthquake cycles, but rather two or so) is still open, and there are signs that perhaps at least in some cases asperities are not stationary. Leaving aside the stationarity of asperities in continental environments, there is very little evidence pro

or con coming from subduction zones. The only work dealing with this issue is *Boyd et al.* [1995], who compared estimated asperity locations of the Aleutian 1957 great earthquake and the 1986 Andreanof Islands event that ruptured the same segment. The authors suggest that asperities were not in the same place, although this conclusion must be regarded cautiously. The data for at least the earlier event would not seem to support a precise enough determination of asperity locations to reach a definite conclusion, and different slip inversions discussed for the 1986 event [*Boyd et al.*, 1995] are not in close agreement.
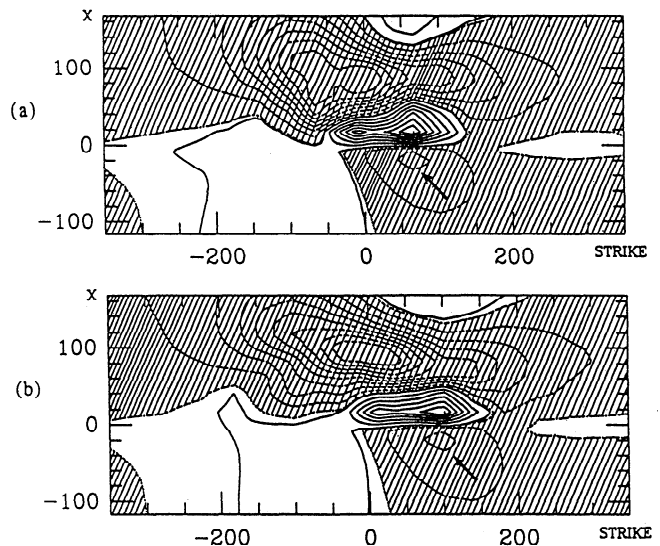

Figure 16. Change σ_{zx} in right-lateral shear stress, negative (left-lateral) where cross-hatched, due to oblique earthquake slip at 45° by amount D on an asperity. (a) For symmetric asperity of Figure 5a, the same case as that for which the extensional stress changes are shown in Figure 11; the contour intervals are $\Delta\sigma_{zx}$ W / μ D = 0.015. (b) For skewed asperity of Figure 12a, strung out in the direction of oblique motion, the case for which extensional stress changes are shown in Figure 12b; the contour intervals are $\Delta\sigma_{zx}$ W / μ D = 0.016.

That case being the only one as for now, we are left with the possibility that if asperities are caused by subduction of seamounts or other topographic irregularities, or by kinks in the interplate interface, then it is likely that they are stationary over many cycles. This is an important issue for predicting the areas of highest seismic moment release, and likely nucleation sites, in future earthquakes, so that any means of improving our understanding of how such areas could be identified, and if they will be stable in time, are of interest.

Only in the last few years has it been realized that the character of the subducting plate greatly influences the structure of continental margins. Recent work by *von Huene and Fluh* [1994], on the Middle America Trench off Costa Rica, reveals the relation between the topography of the subducting oceanic plate and the structure of the margin. Along the coast of Costa Rica three different segments are clearly recognized: A relatively simple first order morphology characterizes the Nicoya margin where smooth oceanic crust subducts. The Osa segment of the margin is broadly uplifted and arched above the broad topography of the subducting Cocos Ridge. Finally, the Quepos margin topography is disrupted opposite the subducting seamount domain and shows seamounts in various stages of subduction and their impact on the structure of the margin. Here we could learn what is a bathymetric signature of a subducted seamount. Assuming that such signatures can be detected even in less detailed bathymetric profiles than the ones available in Costa Rica, one could investigate a possible relation between such signatures and either the known asperities of large earthquakes or, even, segments of plate margins that contain epicenters of largest earthquakes. (The latter would increase the data set, by inclusion of historic earthquakes, and might be interesting as we would be assuming, perhaps quite plausibly, that the epicenter-containing segments generally coincide with asperities. The fact that such segments are indeed different has been proved by *McCaffrey* [1994], who showed that they behave in a more rigid way than other segments.) Here we would assume that asperities could be created by the subducted seamounts in a way described by *Cloos and Shreve* [1994, and manuscript in preparation, 1995].

Another issue that is relevant, assuming that at least some of the asperities are created by subducted seamounts, is the relation between the known asperities or, again, convergent margin segments that include epicenters of historic earthquakes, and topographic heights caused by the subducted seamounts, as observed for the Java Trench by *Masson et al.* [1990], and for the Japan Trench by French and Japanese workers [see *Masson et al.*, 1990]. Though very speculative, if proved, relations between bathymetry signatures and asperities and/or topographic heights and asperities would give a tool in finding asperities in areas with unknown detailed history of seismic release.

A final area of investigation is to see if there is a relation between the number, or perhaps density, of outer-rise faults as observed by detailed geophysical investigations of convergent margins and the amount of seismic slip released in known earthquakes along such margins. This would perhaps relate more to general "strength of seismic coupling" than to individual asperities. Such a relation would follow from the assumption that the outer-rise adjacent to the zones of stronger coupling and seismic

moment release undergoes larger stress variations in general by comparison with less coupled segments, where perhaps the interplate interface deforms in either smaller earthquakes or partially aseismically. We have compared a detailed map of outer slope fault patterns from the western and central Aleutians (Figure 17) [from *Mortera-Gutierrez*, 1995; see also *Mortera-Gutierrez et al.*, 1994] with the areas of seismic moment release for the 1957 Great Aleutian earthquake, as retrieved from body, surface and tsunami waves by *Johnson et al.* [1994], and the Rat Islands 1965 seismic moment inversion by *Christensen and Beck* [1994]. The area of major moment release in 1957, as judged by *Johnson et al.* [1994, Figure 18], covers the strip between approximately 173°W and 179°E and abuts the largest asperity of the 1965 Rat Island event at 177°E to 179°E [*Christensen and Beck*, 1994]. This is precisely the area in Figure 17 with the largest number of faults in the outer rise zone, as compared with zones both east and west of it, which in recent history had smaller seismic moment release (smaller seismic coupling). So this may also be a promising route to understanding structural and tectonic signatures of coupling. Still, we cannot presently dismiss the possibility that the correlation is instead due to a chance coincidence of some preexisting seafloor fault fabric with the zone of strong coupling.

Conclusion

Our work is motivated by two sets of seismic observations. First, *Lay et al.* [1989], as in Figure 1, and others showed that the timing of seismicity in the outer rise and in the slab at intermediate depth is related to stress fluctuations associated with large underthrusting events. Second, *Dmowska and Lovison* [1992] showed, as illustrated in our Figures 3 and 10, that such seismicity is clustered along strike in association with asperities. Those asperities are regions of greatest slip in the underthrusting event. We assumed that those asperity zones are the locations of firmest coupling along the thrust interface, that is, of lowest interseismic slip rate, with the regions outside releasing moment throughout the earthquake cycle in some combination of aseismic creep and moderate seismicity. Using simplified three-dimensional finite element modeling of such heterogeneous coupling, we then examined stress fluctuations in the earthquake cycle and, focusing on the outer rise, found that the stress patterns were consistent with clustering of outer rise seismicity in association with asperities. For the strongly oblique subduction margin of the Rat Islands, western Aleutians, 1965 event, the active areas of the outer rise and slab at intermediate depth are offset along strike (Figure 10, for the outer rise) from asperity locations. We found that offsets like those shown could be explained from the modeling if we assumed that the asperity zones along the thrust interface are strung out along the direction of oblique slip, perhaps reflecting the contact path of subducting seamounts or geometric irregularities along the interface. Shear stress patterns created in the upper plate, when there is oblique subduction, suggest that favorable areas for induction of back-arc strike slip activity following underthrusting, like in the Adak Island, central Aleutians, region of the 1986 Andreanof Island earthquake [*Ekström and Engdahl*, 1989], will also be shifted along
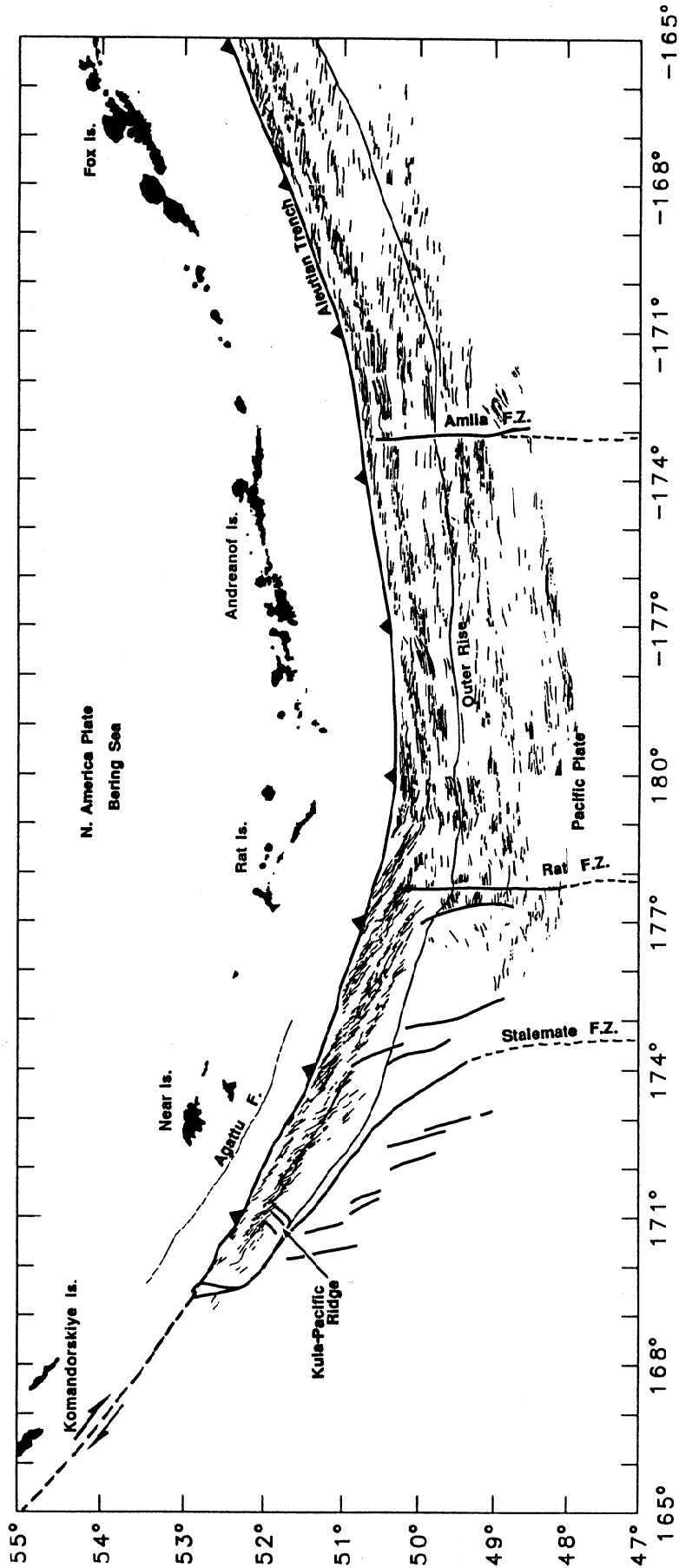
Figure 17. From *Mortera-Gutierrez* [1995]: Seaward slope faults in the Pacific Plate along the Aleutian Trench.

strike from asperity locations. Our analyses show further how deformation patterns on the Earth's surface above asperities differ from those above non-asperities. Such results may provide the background to devise geodetic campaigns to identify inhomogeneous coupling from along-strike variability in deformation observations.

References

Astiz, L., T. Lay, and H. Kanamori, Large intermediate depth earthquakes and the subduction process, *Phys. Earth Planet. Inter.*, 53, 80-166, 1988.

Beck, S. L., and D. H. Christensen, Rupture process of the February 4, 1965, Rat Islands earthquake, *J. Geophys. Res.*, 96, 2205-2201, 1991.

Boyd, T. M., E. R. Engdahl, and W. Spence, Seismic cycles along the Aleutian arc: Analysis of seismicity from 1957 through 1991, *J. Geophys. Res.*, 100, 621-644, 1995.

Christensen, D. H., and S. L. Beck, The rupture process and tectonic implications of the great 1964 Prince William Sound earthquake, *Pure Appl. Geophys.*, 142, 29-53, 1994.

Christensen, D. H., and L. J. Ruff, Outer-rise earthquakes and seismic coupling, *Geophys. Res. Lett.*, 10, 697-700, 1983.

Christensen, D. H., and L. J. Ruff, Rupture process of the March 3, 1985 Chilean earthquake, *Geophys. Res. Lett.*, 13, 721-724, 1986.

Christensen, D. H., and L. J. Ruff, Seismic coupling and outer-rise earthquakes, *J. Geophys. Res.*, 93, 13421-13444, 1988.

Cloos, M., Thrust-type subduction-zone earthquakes and seamount asperities: A physical model for seismic rupture, *Geology*, 20, 601-604, 1992.

Cloos, M., and R. L. Shreve, Subduction channel model for accretion, sediment subduction, and tectonic erosion at convergent plate margins: Seamount asperities and thrust-type subduction zone seismicity, paper presented at SUBCON, An Interdisciplinary Conference on the Subduction Process, USGS, JOI/USSAAC, and NSF, Catalina Island, Calif., June 12-17, 1994.

Dmowska, R., and L. C. Lovison, Intermediate-term seismic precursors for some coupled subduction zones, *Pure Appl. Geophys.*, 126, (N. 2-4), 643-664, 1988.

Dmowska, R., and L. C. Lovison, Seismic behavior of the outer-rise (abstract), *Eos Trans. AGU*, 71, 1468, 1990.

Dmowska, R., and L. C. Lovison, Influence of asperities along subduction interfaces on the stressing and seismicity of adjacent areas, *Tectonophysics*, 211, 23-43, 1992.

Dmowska, R., J. R. Rice, L. C. Lovison, and D. Josell, Stress transfer and seismic phenomena in coupled subduction zones during the earthquake cycle, *J. Geophys. Res.*, 93, 7869-7884, 1988.

Dmowska, R., G. Zheng, J. R. Rice, and L. C. Lovison-Golob, Stress transfer, seismic phenomena and seismic potential in the Shumagin seismic gap, Alaska, paper presented at Wadati Conference on Great Subduction Earthquakes, Geophysical Institute, Univ. of Alaska, Fairbanks, 1992.

Ekström, G., and E. R. Engdahl, Earthquake source parameters and stress distribution in the Adak Island region of the central Aleutian Islands, Alaska, *J. Geophys. Res.*, 94, 15499-15519, 1989.

Goetze, C., and B. Evans, Stress and temperature in the bending lithosphere as constrained by experimental rock mechanics, *Geophys. J. R. Astron. Soc.*, 59, 463-478, 1979.

Johnson, J. M., Y. Tanioka, L. J. Ruff, K. Satake, H. Kanamori, and L. R. Sykes, The 1957 Great Aleutian earthquake, *Pure Appl. Geophys.*, 142, 3-28, 1994.

Lay, T., L. Astiz, H. Kanamori, and D. H. Christensen, Temporal variation of large interplate earthquakes in coupled subduction zones, *Phys. Earth Planet. Inter.*, 54, 258-312, 1989.

Masson, D. G., Fault patterns at outer trench walls, *Mar. Geophys. Res.*, 13, 209-225, 1991.

Masson, D. G., L. M. Parson, J. Milsom, G. Nichols, N. Sikumbang, B. Dwiyanto, and H. Kallagher, Subduction of seamounts at the Java Trench: a view with a long-range sidescan sonar, *Tectonophysics*, 185, 51-65, 1990.

Mendoza, C., S. Hartzell, and T. Monfret, Wide-band analysis of the 3 March 1985 central Chile earthquake: Overall source process and rupture history, *Bull. Seismol. Soc. Am.*, 84, 269-283, 1994.

McAdoo, D. C., J. G. Caldwell, and D. L. Turcotte, On the elastic-perfectly plastic bending of the lithosphere under generalized loading with application to the Kuriles trench, *Geophys. J. R. Astron. Soc.*, 54, 11-26, 1978.

McCaffrey, R., Global variability in subduction thrust zone-forearc systems, *Pure Appl. Geophys.*, 142, 173-224, 1994.

McNutt, M. K., and H. W. Menard, Constraints on yield strength in the oceanic lithosphere derived from observations of flexure, *Geophys. J. R. Astron. Soc.*, 71, 363-394, 1982.

Mortera-Gutierrez, C. A., Seaward slope faults in the Pacific Plate along the Aleutian Trench, Ph.D. Thesis, Department of Geology and Geophysics, Texas A&M University, College Station, TX, September 1995.

Mortera-Gutierrez, C. A., R. L. Carlson, and D. W. Scholl, Accommodation of stresses along the Western Aleutian trench: Inferences from outer-slope fault patterns paper presented at SUBCON, An Interdisciplinary Conference on the Subduction Process, USGS, JOI/USSAAC, and NSF, Catalina Island, Calif., June 12-17, 1994.

Rice, J. R., and W. D. Stuart, Stressing in and near a strongly coupled subduction zone during the earthquake cycle (abstract), *EOS Trans. AGU*, 70, 1063, 1989.

Taylor, M. A. J., G. Zheng, J. R. Rice, W. D. Stuart, and R. Dmowska, Cyclic stressing and seismicity at strongly coupled subduction zones, *J. Geophys. Res.*, in press, 1996.

Trehu, A. M., I. Asudeh, T. M. Brocher, J. H. Luetgert, W. D. Mooney, J. L. Nabelek, and Y. Nakamura, Crustal architecture of the Cascadia forearc, *Science*, 266, 237-243, 1994.

von Huene, R., and E. R. Fluh, A review of marine geophysical studies along the Middle America Trench off Costa Rica and the problematic seaward terminus of continental crust, report, pp. 143-159, GEOMAR, Stuttgart, Germany, 1994.

Wang, K., H. Dragert and H. J. Melosh, Finite element study of uplift and strain across Vancouver Island, *Can. J. Earth Sci.*, 31, 1510-1522, 1994.

Zheng, G., R. Dmowska and J. R. Rice, Modeling earthquake cycles in the Shumagins subduction segment, Alaska, with seismic and geodetic constraints, *J. Geophys. Res.*, in press, 1996.

R. Dmowska, J. R. Rice, and G. Zheng, Division of Applied Sciences, and Department of Earth and Planetary Sciences, Harvard University, Cambridge, MA 02138. (e-mail: dmowska@geophysics.harvard.edu; rice@esag.harvard.edu; zheng@husm.harvard.edu)